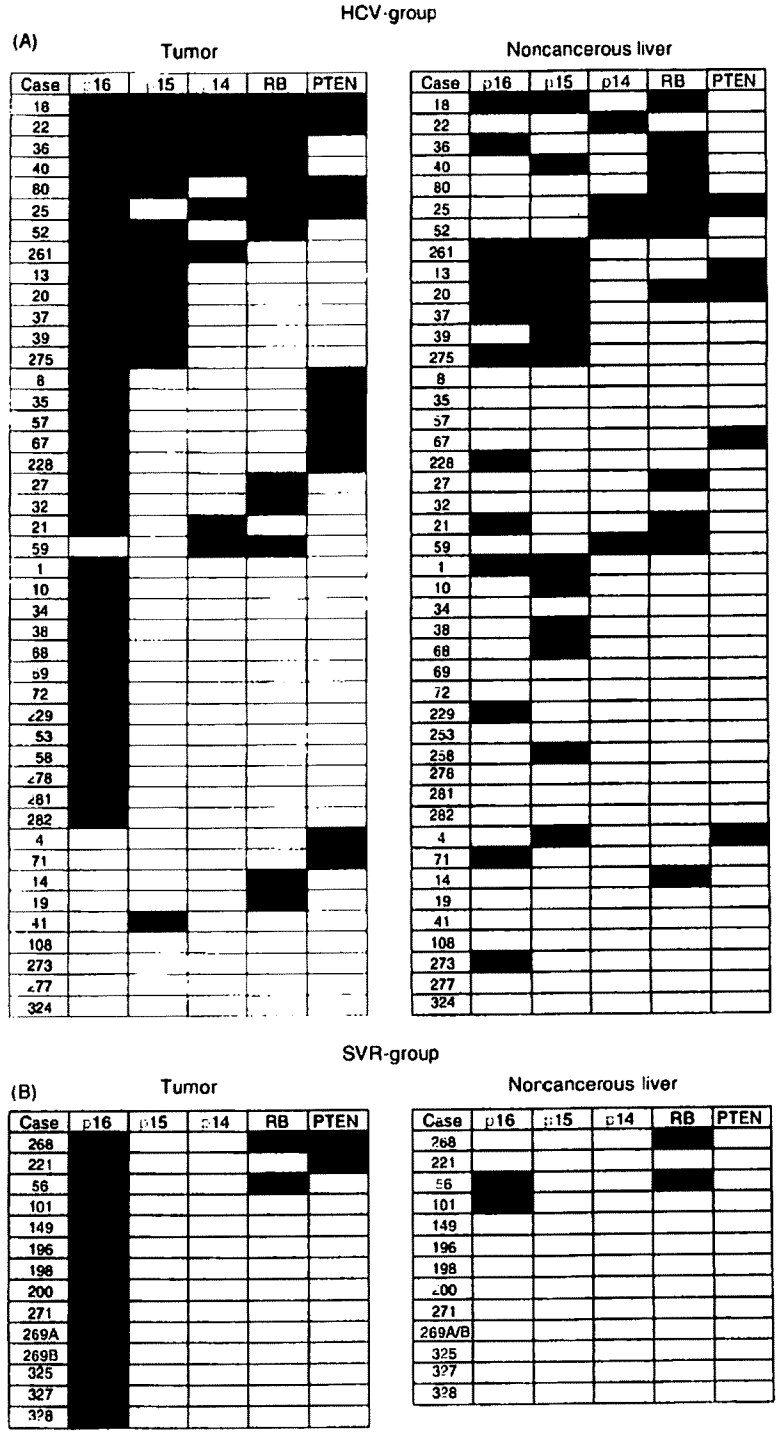

Fig. 1. Methylation patterns of *p16*, *p15*, *p14*, *RB* and *PTEN* promoter in 44 hepatocellular carcinomas (HCCs) and 44 noncancerous liver samples from the hepatitis C virus (HCV) group were examined by methylation-specific polymerase chain reaction (MSP) (A). Methylation patterns were also examined by MSP for 14 HCCs and 13 noncancerous liver samples from the sustained virological response (SVR) group (B). Black boxes indicate methylated sequences, whereas blank boxes indicate unmethylated sequences.

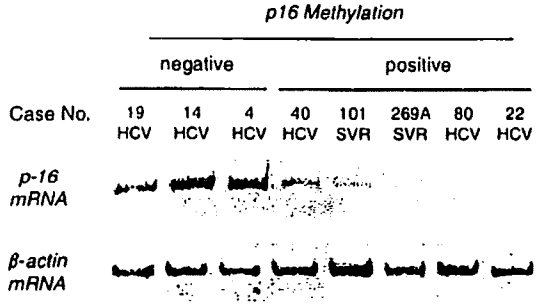

Fig. 2. Expression of *p16* mRNA in hepatocellular carcinoma (HCC). The promoter of *p16* was methylated in cases 40, 101, 269A, 80 and 22. In these tumours, *p16* expression was lower than that in HCC without methylation. β-actin expression was examined as a control. HCV, hepatitis C virus; SVR, sustained virological response.

p14, *RB* and *PTEN* are, respectively, methylated in 58–82% (4, 5, 28–32), 5–64% (5, 32–34), 0–36% (5, 32), 21% (5) and 17% (28) of HCCs from patients with viral infections. In our study, methylation of *p16*, *p15*, *p14*, *RB* and *PTEN* was, respectively, detected in 34 (77.3%), 13 (29.5%), eight (18.2%), 12 (27.3%) and 11 (25.0%) of 44 HCV-HCCs. Our findings are thus consistent with those of previous studies. In SVR-HCC, *p16* was methylated in all samples, whereas *RB* and *PTEN* were methylated in only two samples and methylation of *p15* and *p14* was not detected. This was a novel methylation profile that differed from that of SVR-HCC and HCV-HCC. We showed that promoter methylation of the *p16* gene, leading to the loss of *p16* expression, was frequently observed not only in HCV-HCC but also in SVR-HCC. These data suggested that aberrant *p16* methylation might contribute to the development of SVR-HCC.

Epidemiological studies have shown that past exposure to *Helicobacter pylori* is closely associated with an increased risk of gastric cancer and that most cases of *H. pylori*-negative gastric cancer have a history of exposure to *H. pylori* (35, 36). Maekita and colleagues reported that permanent methylation of specific CpG islands in gastric mucosae is associated with a heightened risk of gastric cancer in *H. pylori*-negative patients (37, 38). It was speculated that methylation of CpG islands in gastric stem cells led to a continuous high level of methylation in gastric mucosae (39). It was well known that HCV was spontaneously eradicated in 20% of patients with the acute infection (40). To our knowledge, there has been no report about HCC development in patients who had been cured in acute hepatitis. In the present study, *p16* was methylated in both HCC infected with HCV and HCC after eradication of HCV. We speculate that *p16* in hepatic stem cells might be methylated in the continuous presence of HCV. These cells with methylated *p16* might survive and grow after eradication of HCV by IFN therapy. Future studies should examine the methylation status of genes in successive liver specimens obtained before and after IFN therapy.

In conclusion, epigenetic alterations of some genes in SVR-HCC differed from those in HCV-HCC. Moreover, mutation of mtDNA was less common in SVR-HCC than in HCV-HCC. The present results suggest that the development of HCC in patients cured of HCV infection by IFN therapy might be associated with particular molecular alterations.

Acknowledgements

We acknowledge Ms Mayumi Shinzaki for her excellent technical assistance. This study was supported in part by a grant-in-aid from the Japan Society of the Promotion of Science (no. 16590619 to A. T.).

References

1. Marrogi AJ, Khan MA, van Gijssel HE, *et al.* Oxidative stress and p53 mutations in the carcinogenesis of iron overload-associated hepatocellular carcinoma. *J Natl Cancer Inst* 2001; 93: 1652–5.
2. Nishikawa M, Nishiguchi S, Shiomi S, *et al.* Somatic mutation of mitochondrial DNA in cancerous and noncancerous liver tissue in individuals with hepatocellular carcinoma. *Cancer Res* 2001; 61: 1843–5.
3. Minouchi K, Kaneko S, Kobayashi K. Mutation of p53 gene in regenerative nodules in cirrhotic liver. *J Hepatol* 2002; 37: 231–9.
4. Kaneto H, Sasaki S, Yamamoto H, *et al.* Detection of hypermethylation of the p16 (INK4A) gene promoter in chronic hepatitis and cirrhosis associated with hepatitis B or C virus. *Gut* 2001; 48: 372–7.
5. Roncalli M, Bianchi P, Bruni B, *et al.* Methylation framework of cell cycle gene inhibitors in cirrhosis and associated hepatocellular carcinoma. *Hepatology* 2002; 36: 427–32.
6. Moriya K, Fujie H, Shintani Y, *et al.* The core protein of hepatitis C virus induces hepatocellular carcinoma in transgenic mice. *Nat Med* 1998; 4: 1065–7.
7. Majumder M, Ghosh AK, Steele R, *et al.* Hepatitis C virus NS5A physically associates with p53 and regulates p21/waf1 gene expression in a p53-dependent manner. *J Virol* 2001; 75: 1401–7.
8. Larsson M, Babcock E, Grakoui A, *et al.* Lack of phenotypic and functional impairment in dendritic cells from chimpanzees chronically infected with hepatitis C virus. *J Virol* 2004; 78: 6151–61.
9. McHutchison JG, Gordon SC, Schiff ER, *et al.* Interferon alfa-2b alone or in combination with ribavirin as initial treatment for chronic hepatitis C. Hepatitis Interventional Therapy Group. *N Engl J Med* 1998; 339: 1485–92.
10. Manns MP, McHutchison JG, Gordon SC, *et al.* Peginterferon alfa-2b plus ribavirin compared with interferon alfa-2b plus ribavirin for initial treatment of chronic hepatitis C: a randomised trial. *Lancet* 2001; 358: 958–65.
11. Bruno S, Stroffolini T, Colombo M, *et al.* Sustained virological response to interferon-alpha is associated with improved outcome in HCV-related cirrhosis: a retrospective study. *Hepatology* 2007; 45: 579–87.
12. Yoshida H, Shiratori Y, Moriyama M, *et al.* Interferon therapy reduces the risk for hepatocellular carcinoma: national surveillance program of cirrhotic and noncirrhotic patients with chronic hepatitis C in Japan. IHIT Study Group. Inhibition of Hepatocarcinogenesis by Interferon Therapy. *Ann Intern Med* 1999; 131: 174–81.
13. Toyoda H, Kumada T, Tokuda A, *et al.* Long-term follow-up of sustained responders to interferon therapy, in patients with chronic hepatitis C. *J Viral Hepat* 2000; 7: 414–9.
14. Enokimura N, Shiraki K, Kawakita T, *et al.* Hepatocellular carcinoma development in sustained viral responders to interferon therapy in patients with chronic hepatitis C. *Anticancer Res* 2003; 23: 593–6.
15. Makiyama A, Itoh Y, Kasahara A, *et al.* Characteristics of patients with chronic hepatitis C who develop hepatocellular carcinoma after a sustained response to interferon therapy. *Cancer* 2004; 101: 1616–22.
16. Tamori A, Nishiguchi S, Shiomi S, *et al.* Hepatitis B virus DNA integration in hepatocellular carcinoma after interferon-induced

disappearance of hepatitis C virus. *Am J Gastroenterol* 2005; 100: 1748–53.
17. Radkowski M, Gallegos-Orozco JF, Jablonska J, *et al.* Persistence of hepatitis C virus in patients successfully treated for chronic hepatitis C. *Hepatology* 2005; 41: 106–14.
18. Tamori A, Yamanishi Y, Kawashima S, *et al.* Alteration of gene expression in human hepatocellular carcinoma with integrated hepatitis B virus DNA. *Clin Cancer Res* 2005; 11: 5821–6.
19. Desmet VJ, Gerber M, Hoofnagle JH, *et al.* Classification of chronic hepatitis: diagnosis, grading and staging. *Hepatology* 1994; 19: 1513–20.
20. King MP, Attardi G. Human cells lacking mtDNA: repopulation with exogenous mitochondria by complementation. *Science* 1989; 246: 500–3.
21. Hayashi H, Sugio K, Matsumata T, *et al.* The clinical significance of p53 gene mutation in hepatocellular carcinomas from Japan. *Hepatology* 1995; 22: 1702–7.
22. Herman JG, Graff JR, Myohanen S, *et al.* Methylation-specific PCR: a novel PCR assay for methylation status of CpG islands. *Proc Natl Acad Sci USA* 1996; 93: 9821–96.
23. Zysman MA, Chapman WB, Bapat B. Considerations when analyzing the methylation status of PTEN tumor suppressor gene. *Am J Pathol* 2002; 160: 795–800.
24. To KF, Leung WK, Lee TL, *et al.* Promoter hypermethylation of tumor-related genes in gastric intestinal metaplasia of patients with and without gastric cancer. *Int J Cancer* 2002; 102: 623–8.
25. Tamori A, Nishiguchi S, Nishikawa M, *et al.* Correlation between clinical characteristics and mitochondrial D-loop DNA mutations in hepatocellular carcinoma. *J Gastroenterol* 2004; 39: 1063–8.
26. Nishikawa M, Nishiguchi S, Kioka K, *et al.* Interferon reduces somatic mutation of mitochondrial DNA in liver tissues from chronic viral hepatitis patients. *J Viral Hepat* 2005; 12: 494–8.
27. Huang LR, Hsu HC. Cloning and expression of CD24 gene in human hepatocellular carcinoma: a potential early tumor marker gene correlates with p53 mutation and tumor differentiation. *Cancer Res* 1995; 55: 4717–21.
28. Schagdarsurengin U, Wilkens L, Steinemann D, *et al.* Frequent epigenetic inactivation of the RASSF1A gene in hepatocellular carcinoma. *Oncogene* 2003; 22: 1866–71.
29. Matsuda Y, Ichida T, Matsuzawa J, *et al.* p16(INK4) is inactivated by extensive CpG methylation in human hepatocellular carcinoma. *Gastroenterology* 1999; 116: 394–400.
30. Liew CT, Li HM, Lo KW, *et al.* High frequency of p16INK4A gene alterations in hepatocellular carcinoma. *Oncogene* 1999; 18: 789–95.
31. Li X, Hui AM, Sun L, *et al.* p16INK4A hypermethylation is associated with hepatitis virus infection, age, and gender in hepatocellular carcinoma. *Clin Cancer Res* 2004; 10: 7484–9.
32. Fukai K, Yokosuka O, Imazeki F, *et al.* Methylation status of p14ARF, p15INK4b, and p16INK4a genes in human hepatocellular carcinoma. *Liver Int* 2005; 25: 1209–16.
33. Jin M, Piao Z, Kim NG, *et al.* p16 is a major inactivation target in hepatocellular carcinoma. *Cancer* 2000; 89: 60–8.
34. Wong IH, Lo YM, Yeo W, *et al.* Frequent p15 promoter methylation in tumor and peripheral blood from hepatocellular carcinoma patients. *Clin Cancer Res* 2000; 6: 3516–21.
35. Forman D, Webb P, Parsonnet J. *H. pylori* and gastric cancer. *Lancet* 1994; 343: 243–4.
36. Forman D, Newell DG, Fullerton F, *et al.* Association between infection with *Helicobacter pylori* and risk of gastric cancer: evidence from a prospective investigation. *BMJ* 1991; 302: 1302–5.
37. Maekita T, Nakazawa K, Mihara M, *et al.* High levels of aberrant DNA methylation in *Helicobacter pylori*-infected gastric mucosae and its possible association with gastric cancer risk. *Clin Cancer Res* 2006; 12: 989–95.
38. Tatematsu M, Tsukamoto T, Mizoshita T. Role of *Helicobacter pylori* in gastric carcinogenesis: the origin of gastric cancers and heterotopic proliferative glands in Mongolian gerbils. *Helicobacter* 2005; 10: 97–106.
39. Ushijima T, Nakajima T, Maekita T. DNA methylation as a marker for the past and future. *J Gastroenterol* 2006; 41: 401–7.
40. Alter MJ. Epidemiology of hepatitis C in the West. *Semin Liver Dis* 1995; 15: 5–14.

Available online at www.sciencedirect.com
ScienceDirect
Comparative Immunology, Microbiology & Infectious Diseases 31 (2008) 435–448
COMPARATIVE IMMUNOLOGY MICROBIOLOGY & INFECTIOUS DISEASES
www.elsevier.com/locate/cimid

Comparative aspects on the role of polypyrimidine tract-binding protein in internal initiation of hepatitis C virus and picornavirus RNAs

T. Nishimura[a,e], M. Saito[a], T. Takano[a,b,c], A. Nomoto[d], M. Kohara[b], K. Tsukiyama-Kohara[a,b,c,*]

[a]*Department of Experimental Phylaxiology, Faculty of Medical and Pharmaceutical Sciences, Kumamoto University 1-1-1, Honjo, Kumamoto 860-8556, Japan*
[b]*Department of Microbiology and Cell Biology, The Tokyo Metropolitan Institute of Medical Science, Tokyo 113-8613, Japan*
[c]*Laboratory Animal Research Center, Institute of Medical Science, The University of Tokyo, Tokyo 108-8639, Japan*
[d]*Graduate School of Medicine, The University of Tokyo, Tokyo 113-0033, Japan*
[e]*The Chemo-Sero-Therapeutic Research Institute, Tokyo 869-1298, Japan*

Accepted 6 July 2007

Abstract

We compared the effects of polypyrimidine tract-binding protein (PTB) on hepatitis C virus (HCV genotype IIa), encephalomyocarditis virus (EMCV) and poliovirus internal ribosome entry site (IRES) activities *in vitro*. It bound strongly to EMCV IRES, but weakly to PV and HCV RNAs. PV IRES showed the strongest dependency to PTB and it showed less than one-tenth of IRES activity after the immuno-depletion of PTB from HeLa S10 lysate with pre-coated anti-PTB IgG beads, comparing to the normal IgG beads-treated S10 lysate. EMCV IRES activity was approximately 40% of that of normal control after PTB depletion.

*Corresponding author. Department of Experimental Phylaxiology, Faculty of Medical and Pharmaceutical Sciences, Kumamoto University 1-1-1, Honjo, Kumamoto 860-8556, Japan.
Tel./fax: +81 96 373 5560.
E-mail address: kkohara@kumamoto-u.ac.jp (K. Tsukiyama-Kohara).

0147-9571/$ - see front matter
doi:10.1016/j.cimid.2007.07.002

Especially, HCV IRES activity was approximately 95%, and most weekly affected by the depletion of PTB. Repletion of PTB to depleted S10 lysate restored activities of PV and EMCV IRESs. The data suggest that PTB plays an important role in picornaviral IRESs, but not in HCV IRES.

Keywords: PTB; HCV; IRES; EMCV; PV; HeLa

Résumé

Dans notre étude, nous avons comparé les effet de la 'polypyrimidine track-binding' (PTB) virus de l'hépatite C (génotype IIa) et l'activité du virus encéphalomyodardite (EMCV) et de l'IRES du poliovirus *in vitro*. La PTB se fixe de manière résistante à l'IRES de l'EMCV mais de manière fragile à l'ARN du PV et du VHC. L'IRES du PV montre la dépendance la plus forte à la PTB et il montre une activité d'IRES de moins de un dixième après immuno-déplétion de la PTB du lysat HeLa10 par des billes d'IgG anti-PTB prêtes à l'emploi, par rapport au HeLa10 traité par des billes d'IgG normales. L'activité de l'IRES de l'EMCV était approximativement égale à 40% de celle sous contrôle normal après déplétion de la PTB. L'activité de l'IRES du VHC était approximativement égale à 95% et la moins sensible à la déplétion de la PTB. La réplétion de la PTB au lysat S10 appauvri rétablit les activités des IRES du PV et de l'EMCV. Les données suggèrent que la PTB joue un rôle important dans les IRES picornaviraux mais pas dans les IRES du VHC. De plus,

Mots clés: PTB; VHC; PTB; IRES; PV; HeLa

1. Introduction

Hepatitis C virus (HCV) possesses a single-stranded RNA (approximately 9610 nucleotides), and classified into the family *Flaviviridae* [1–4]. HCV is a major causative agent of non-A non-B hepatitis, and likely progresses into the chronic hepatitis, cirrhosis and hepatocellular carcinoma.

The 5′ untranslated region (5′UTR) of HCV RNA genome is 341 nucleotides and an internal ribosome entry site (IRES) has been proven to exist in this region [5]. Activities of IRESs of HCV were different from each genotype, and genotype IIa showed almost two-fold higher IRES activity than genotype Ib [6,7].

The IRESs have been discovered in the *Picornavirus* genomes and have a complex RNA secondary structure [5,8]. The importance of secondary structure to IRES function is understood by studies that sequence substitutions within the IRES are accompanied by compensatory mutations that act to maintain the RNA secondary structure. The 40S ribosome subunit is recruited within these IRES without binding to the m^7G cap and eIF4E [9,10]. IRESs can be classified into at least 3 groups, according to their features. IRESs derived from entero- and rhinoviruses are classified into type 1(poliovirus), and oligopyrimidine tract is located in 50–100 nucleotides past the 3′ end of the IRES [11,12]. The oligopyrimidine tract

immediately follows the 3′ end of type 2 (cardio- and aphthoviruses) IRES. Encephalomyocarditis virus (EMCV) and foot and mouse disease virus possess type 2 IRESs and utilyzes eIF4G and 4B [13,14]. The HCV and classical swine fever virus (CSFV) possess type 3 IRESs which interact directly to 40S ribosome subunit and eIF3 [15]. In addition to the requirement for eIF in each IRESs, the existence of internal initiation trans-acting factors (ITAFs) has been reported [16,17]. One of ITAFs binds to picornavirus and HCV IRES commonly is polypyrimidine tract-binding protein (PTB) [11,18–20]. PTB may work in each IRESs, however, its exact role in internal initiation has been still unclear at present. In the present study, requirement of PTB in poliovirus, EMCV and HCV IRESs has been characterized, and compared in *in vitro* translation system by depletion and complementation of PTB.

2. Materials and methods

2.1. Isolation of cDNA clones and construction of expression vectors

HCV cDNA that corresponds to nucleotide positions 1-418 (GenBank) was isolated by PCR from plasma of HCV type IIa infected patients [5], using a sense primer, 5′-GATCTAGAGCCCGCCCCCTGATGGGGGCGA-3′, and antisense primer 5′-TGTCCTGCAGTTCAAGGGCCC-3′. The amplified cDNA was digested with XbaI and AatII, and replaced with an XbaI and AatII fragment (5′UTR) of pkIV [5]. A whole cDNA which was excised by XbaI-HindIII was filled up with Klenow fragment (Takara) and cloned into StuI site of pNar3 [5], and the resulting plasmid was designated as pNII5′.

Poliovirus cDNA expression vector T7M2, CAT gene with 5′UTR of EMCV (pBSECAT) and T7CAT were constructed, as described previously [19,21].

PTB cDNA that encodes whole coding region (amino acids no. 1-531) [22] or C terminal half (amino acids no. 291-531) of PTB was synthesized by RT-PCR, and cloned into the downstream of glutathione S transferase (GST) protein in frame in pGEX-KG vector, and was designated as pGST-PTB.

2.2. Expression of PTB and production of specific antibodies

The pGST-PTB was transformed in *Esherichia coli* strain SCS-1 and induced expression with 1 mM IPTG induction. *E. coli* culture (40 ml) was peletted by centrifuge and lyzed with lysozyme (1 mg/ml) and sonicated with 1% TritonX100 and 10 mM DTT. The supernatant was reacted to Glutathione Sepharose 4B (Amersham Bioscience), cleaved by thrombin (SIGMA) and purified with ploy U Sepharose 4B (Amersham Bioscience), as described previously [22]. Rabbits or guinea pigs immunized were over four times intradermal and subcutaneously or intraperitonealy with purified recombinant whole or C-terminal half of PTB (200 μg). These hyperimmune sera were purified by the protein G Sepharose 4B (Amersham Bioscience). The anti PTB rabbit IgG was further purified by the affinity

column of PTB cross-linking Formyl Cellulofine (Seikagaku Kogyo Co.), as described by manufacturer's instruction manual.

2.3. UV cross-linking assays and immunoprecipitation

RNA probes corresponding to nucleotide(nt.) 1-341 of the HCV 5′UTR, nt. 260-833 of the EMCV 5′UTR and nt. 1-747 of the PV 5′UTR were generated by the digestion of pNII5′ with BspHI, pBSECAT with BalI and pM1(T7) with HgiAI, respectively, and transcribed by using Megascript™ T7 RNA polymerase kit (Ambion) with [α-^{32}P]UTP (NEN). Labelled RNA probes were purified by the Nuc Trap™ push columns (Stratagene). Probes ($1-5 \times 10^6$ cpm) were incubated with or without competitor RNA in HeLa S10 lysate (10 μg) at 30 °C for 20 min and irradiated on ice for 20 min in a UV Stratalinker (Stratagene). Unbound RNAs were digested with 10 μg of RNase A (Sigma), 200 units of RNase T1 (Gibco BRL) and 1 unit of phosphodiesterase I (Amersham Bioscience). Samples were analyzed by SDS-PAGE and dried gel was exposed to imaging plate (Fuji) or X-ray film (Kodak). Radioactivity was measured by the Bio-image analyzer BAS 2000 (Fuji).

HeLa S10 or recombinant PTB which was UV cross-linked to labeled HCV RNA was solubilyzed by single lysis buffer containing 1% NP40, reacted with affinity-purified anti-PTB Ig (4 μg) and precipitated by affigel protein A (Bio Rad) beads. Precipitated protein was further characterized by SDS-PAGE.

2.4. Immuno-depletion test

Affigel protein A (Bio Rad) 50 μl was pretreated with HeLa S10 100 μl at 37 °C for 1 h. The affinity purified anti-PTB Rabbit IgG (500 μg) was added, and rotated at room temperature for 3 h. These IgG beads were coated by 10% FCS-0.1 M phosphate buffer (pH 8.0) at 37 °C for 1 h, washed with S10 dialysis buffer (10 mM Hepes-KOH pH7.5, 90 mM KOAc, 1.5 mM $Mg(OAc)_2$), and reacted to HeLa S10 lysate (150 μl) at 4 °C overnight. The supernatants of each reaction were utilized for *in vitro* translation.

2.5. Competitive ELISA

Serocluster 'U' vinyl plate with 96 wells (Costar) was coated with affinity purified rabbit anti-PTB-C term IgG (2.5 μg/ml) at 4 °C overnight. After blocking with 1% casein PBS (−) at 25 °C for 2 h, non-treated or immunodepleted HeLa S10 lysate were added to each well, and incubate at 25 °C for 2 h. Purified recombinant PTB was used for standard and non-treated or immunodepleted HeLa S10 lysates were added to each well, and incubate at 25 °C for 2 h. Then anti-PTB guinea pig IgG (1 μg/ml) was reacted at 37 °C for 1 h, and finally anti-guineapig -IgG HRP (Dako 1:2000) was reacted at 37 °C for 1 h. *Ortho*-phenylene diamine was added to each well as substrate, and the absorbance was measured by microplate reader Model 450 (Bio Rad).

2.6. In vitro transcription and translation

Plasmids were linearized by digestion with XmnI (pNII5′), HpaI (pBSECAT) and NheI (p(M1)T7) and transcribed into RNA by Megascript™ T7 RNA polymerase kit (Ambion). RNAs were treated with DNase I, precipitated with LiCl, and quantitated by the Spectrophotometer DU64 (Beckman).

Synthetic RNAs (pNII5′ RNA; 1.0 pmol, pBSECAT; 1.8 pmol, p(M1)T7; 0.36 pmol and they were optimized for the linear phase in translation activity) were translated in HeLa S10 lysates at 37 °C for 30 min with [^{35}S]-Methionine (ICN), as described previously[5] . Translation products were analyzed using 7.5–15% gradient SDS-PAGE.

2.7. Restoration assay

Purified recombinant PTB, bovine serum albumin and ribosome salt wash (RSW) were dialyzed to S10 dialysis buffer, and added to PTB depleted or non-treated HeLa S10. RSW (total 6.7 ml) was prepared from 6.1 l of HeLa S10, as described previously [5] (kindly supplied by Dr. H. Toyoda).

3. Results

3.1. Fifty-seven and 60 kDa doublet protein bound HCV, EMCV and PV RNA

HeLa cytoplasmic proteins that were detected by UV cross-linking to ^{32}P-UTP labeled RNA derived from the HCV, EMCV, and PV 5′UTR were compared (Fig. 1). Total counts of binding proteins in HCV RNA was five times lower than those of EMCV RNA, and three times lower than those of PV-RNA (PSL; HCV 21536.9, EMCV 105622.8, PV 59307.9). Among these cytoplasmic proteins, 57 and 60 kDa doublet bands on HCV RNA,EMCV RNA and PV RNA have been identified to be PTB (Fig. 1, indicated by asterisk). According to band intensities of the 57 and 60 kDa proteins, PTB bound to EMCV IRES most abundantly, and more diminished amount of PTB bound to PV and HCV IRESs (Fig. 1).

3.2. Identification of P57/60 kDa doublet protein on HCV-RNA as PTB

HCV-IRES-binding proteins with molecular weight of 57/60 kDa were further characterized. The recombinant PTB protein was expressed in *E. coli.* in the presence of IPTG, purified by glutathione sepharose and polyU sepharose column (Fig. 2A), and reacted with affinity purified anti-PTB IgG (Fig. 2B), as described in Section 2. Labeled HCV RNA 5′UTR was cross-linked to HeLa S10 lysate, and immunoprecipitated by affinity purified anti-PTB IgG (Fig. 3). The 57 and 60 kDa doublet bands were specifically reacted to the anti-PTB IgG (Fig. 3, lane HeLa). The recombinant PTB protein was cross-linked with HCV RNA 5′UTR and precipitated with anti-PTB IgG (Fig. 3, lane PTB). These results strongly indicate that PTB

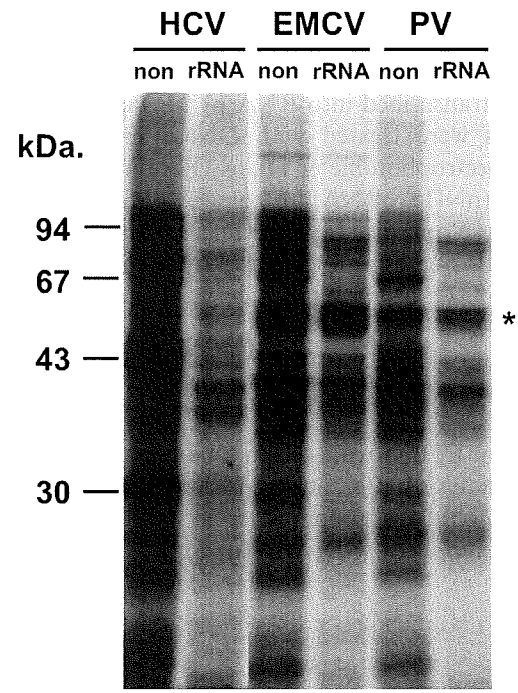

Fig. 1. UV-cross-linking analysis of binding factors to HCV, EMCV and PV-IRES RNAs. Each reaction without competitor indicates "non", and with competitor rRNA indicates rRNA on the top of the lanes. Asterisk indicates the position of PTB proteins. An asterisk indicates PTB binding.

specifically bound to HCV RNA 5′UTR, and observed as doublet protein with molecular weight of 57 and 60 kDa.

3.3. Depletion of PTB in HeLa S10 lysate

Previous results indicated the possibility that other factors than canonical eukaryotic translation initiation factors (eIFs) are working in cap independent translation. PTB is one of the candidates and when the PTB might be commonly used in several kinds of IRESs, it might play the central role in internal initiation. To compare the significance of PTB in translation initiation in HCV and other Picorna virus IRESs, PTB in HeLa S10 lysate was depleted by affinity purified anti-PTB IgG. For the depletion of PTB, pre-coating of Affi-gel protein A beads was necessary to block the non-specific adsorption, as described in Section 2. Pre-coated beads were reacted with anti-PTB IgG. From the preliminary experiments, more than 100 times higher molar ratio of anti-PTB IgG to PTB in S10 lysates was required for the over 90% depletion, as described in Materials and methods. We performed the PTB depletion, and 94.5% of PTB was depleted by anti-PTB IgG and 26.3% of PTB was depleted by pre-immune IgG (Fig. 4). We further examined the effect of PTB

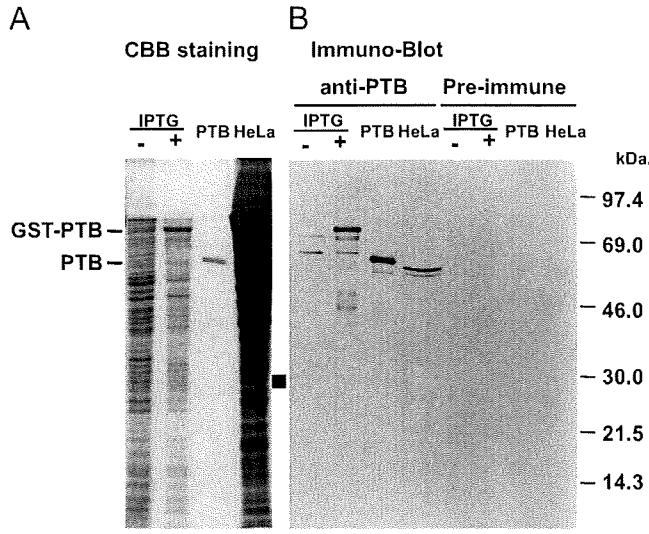

Fig. 2. Expression of recombinant PTB protein fused with GST in *E. coli*: (A) Expression of PTB protein was induced by IPTG, purified by glutathione sepharose column and stained with CBB. (B) Expressed recombinant PTB was transferred to membrane and reacted with specific antibody by WB.

depletion to the binding of cellular factors to three IRESs (Fig. 5). In PTB depleted lysates, binding of 57 and 60 kDa doublet protein was decreased, especially in PV-RNA. However, binding of other factors was not influenced significantly, other than 28 kDa protein (Fig. 5, indicated by an arrow).

3.4. *Effect of PTB depletion in translation*

Influence of PTB depletion was examined in HCV, EMCV and PV-RNA (Fig. 6A, Table 1). The reaction curves of each RNA were different from each other (data not shown), and the optimum quantity of each RNA used in this study was different from each other (Table 1). From the comparison of translation activity in PTB depleted S10 lysates, translation of PV-RNA was significantly decreased in 4 and 8 μl lysates (22–4.5%, 15–0.9%, Table 1, Fig. 6A). Translation of EMCV-IRES was significantly decreased after PTB depletion (53–44% (4 μl), 28–11% (8 μl)), but this suppression was not as much as PV-IRES. Activity of HCV-IRES was almost similar between pre-immune IgG-treated and anti-PTB IgG-treated S10 lysates. Because the optimal RNA quantities for translation are different in each IRESs, therefore, we calculated the ratio of PTB quantity per template RNA molecules (PTB/RNA) (ng/pmol; Table 1). In PV-IRES, translation activity was significantly reduced after depletion (4.5%, 0.9%) and the PTB/RNA ratio was 1.4 and 0.56. EMCV-IRES and HCV-IRES activity. Influence of PTB depletion to HCV-IRES activity was much lower than those of PV and EMCV.

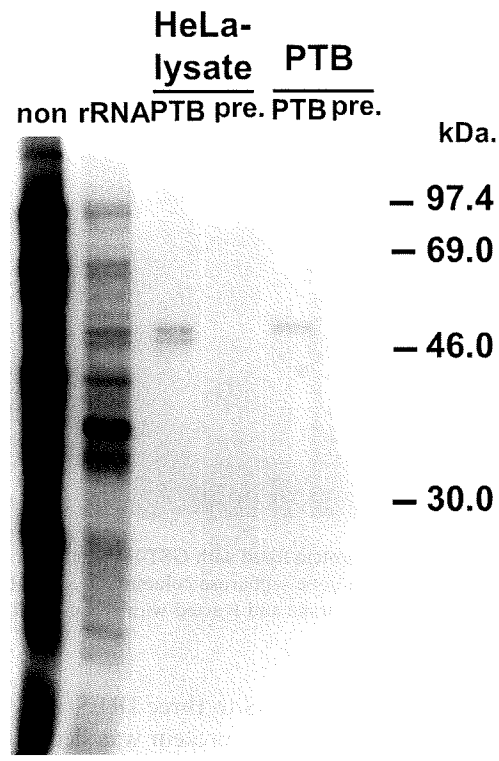

Fig. 3. HCV-IRES cross-linked S10 and PTB was immuno-precipitated by purified anti PTB antibody and pre-immune antibody. The 57 and 60 kDa doublet bands were specifically reacted to the anti-PTB IgG (lane HeLa). The recombinant PTB protein was cross-linked with HCV RNA 5′UTR and precipitated with anti-PTB IgG (lane PTB). Pre-immune antibody did not reacted to both Hela S10 and PTB.

The IRES activity of EMCV and PV-RNA was decreased by treatment of pre-immune IgG, however, treatment of pre-immune IgG did not influence significantly to the IRES activity of HCV-RNA.

3.5. Restoration of PTB to depleted S10

To clarify the effect of immuno-depletion was mainly caused by the decreased quantity of PTB, the purified recombinant PTB or RSW was added to depleted S10 (Fig. 6B). The IRES activity of PV-RNA in depleted S10 lysate (6 μl) was increased by the addition of PTB in dose-dependent manner. The EMCV-IRES activity was recovered even in the presence of 1 μg of PTB in depleted S10 lysate (4.0 μl). When too much quantity of PTB was added to the S10, translation activity of PV, EMCV and HCV decreased (over 10 times of PTB in PV, over 300 times in EMCV and over 500 times in HCV RNA, data not shown).

Translation activity of PV and EMCV-RNA became higher after the addition of RSW to anti-PTB IgG depleted S10 (150% and117%, respectively) (date not

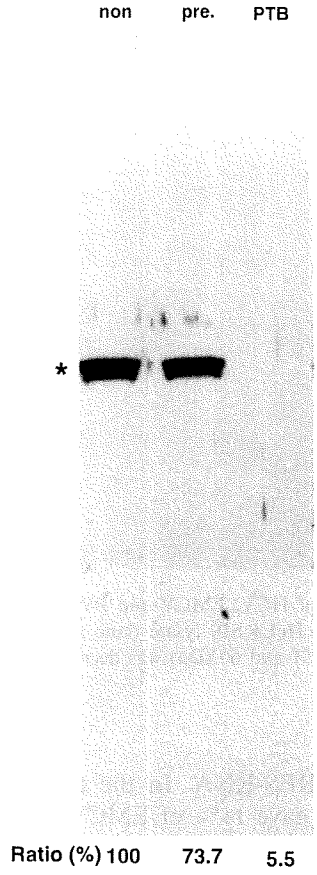

Fig. 4. Depletion of HeLa S10 by pre-immune IgG and affinity purified anti-PTB IgG. They were reacted with anti-PTB antibody by WB. Asterisk indicates the position of PTB proteins. Anti-PTB IgG deplete 94.5% of PTB (lane PTB) and pre-immune IgG deplete 26.3% of PTB (lane pre).

shown). This might indicate the existence of several translation factors other than PTB, which were lost during the treatment of IgG.

Taken together, results of this study strongly indicate that significance of PTB was highest in PV-IRES and was lowest implication in HCV-IRES.

4. Discussion

In present study, the significance of PTB in HCV, EMCV and PV IRESs has been compared. From the immuno-depletion experiment (Table 1), PTB-Ig depleted S10 (4.0 μl) contained 0.009 molecule of PTB per 1 molecule of RNA, in which PV IRES activity is 0.9%. This may indicate that almost one PTB molecule should be required

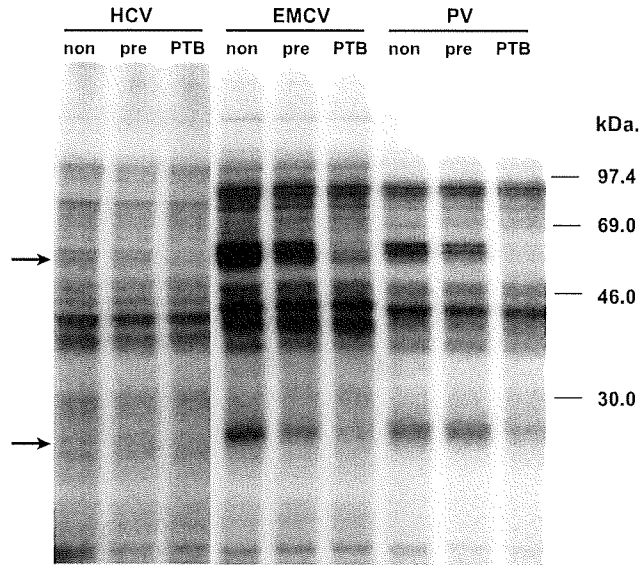

Fig. 5. UV-cross-linking analysis of HCV, EMCV and PV RNA with non-treated, pre-immune IgG-treated, and anti-PTB IgG-treated HeLa S10 lysate (lane non, pre, PTB). Upper arrow indicates the binding of PTB. Doublet protein (57 and 60 kDa) was decreased, especially in PV-RNA. Lower arrow indicates 28 kDa protein.

for 100% activity of PV IRES-RNA. In the case of EMCV IRES-RNA, 0.002 molecule of PTB per RNA gave 11% of EMCV IRES activity, and that of HCV IRES, 0.0025 molecule of PTB gave 31% of HCV IRES activity. Therefore, requirement of PTB for IRES activity was highest in PV, and less in EMCV and HCV IRES-RNA.

From the results in this study, we can compare the requirement amount of PTB in IRES activity with those of canonical eIFs. The most limiting initiation factor in cells is eIF4E, with estimates in rabbit reticulocyte lysates ranging from 0.02 copies [23] to 1 copy [24] per ribosome. The concentration of ribosomes has been estimated to be approximately 2 μM [25]. From the results of *in vitro* translation experiment, PTB should work at 0.1–0.15 M in each IRESs at maximum activity (Table 1). Therefore, working concentration of PTB for IRES activity should show almost similar to those of eIFs.

During the immuno-depletion experiment, treatment of normal IgG conjugated beads decreased the IRESs activity; 89 (6.5 μl) or 33 (3.5 μl)% in HCV IRES, 53 or 28% in EMCV IRES, and 22% or 15% in PV-IRES (Table 1). This may suggest the existence of unknown factors, which could be inactivated during the process of immuno-depletion experiment, and these effects in PV-IRES were highest among the IRESs. PV-IRES is classified into the type I [26], and the canonical eIFs with the exception of cap-binding protein eIF4E [27] and PTB [26], La [26] and 39 kDa poly(rC)-binding protein [26] are working. In EMCV IRES (type II), eIF4G was

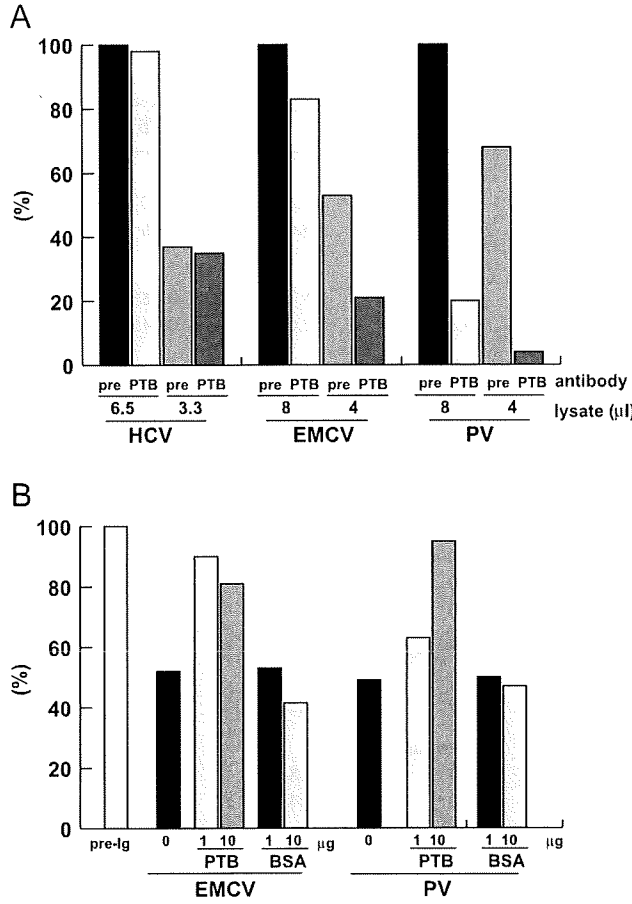

Fig. 6. (A) Effect of PTB depletion in HCV, EMCV and PV IRES. IRESs were translated in pre-immune IgG-depleted and anti-PTB IgG depleted S10 lysates (3.3, 6.5 μl in HCV-IRES, 4.0, 8.0 μl in EMCV- and PV-IRES. Translated products in SDS-PAGE were measured by image analyzer, and the quantity (PSL) of pre-immune IgG-treated S10 lysate was calculated as 100%. (B) Recovery of translation in PTB depleted S10 lysate by addition of recombinant PTB protein (1 and 10 μg. Translated products in SDS-PAGE were measured by image analyzer, and the quantity (PSL) of pre-immune IgG-treated S10 lysate was calculated as 100%.

directly bound and eIF4A and eIF4B can recruit 43S preinitiation complex which is composed of 40S ribosomal subunit and eIF3, eIF2, GTP and initiator tRNA[13]. Recent findings indicated the dependence of EMCV IRES on PTB for activity [28]. The HCV IRES possesses striking difference from type I and II IRESs, it recruits 43S preinitiation complex to initiation codon to form a 48S complex without involvement of eIF4A, 4B or 4F [29]. Thus, HCV IRES is simple and does not require most of eIFs, and might not be influenced by the depletion experiment using normal IgGs.

Table 1
Effect of PTB depletion in HCV, EMCV and PV IRES

RNA	RNA quantity (pmol)	S10 (μl)	PTB (ng)	Molar ratio of PTB to RNA	Ratio of translation (%)[a]
HCV	1.0	*Untreated*			
		6.5	7.2	0.12	100
		3.5	3.6	0.06	63
		Pre-im.-IgG			
		6.5	5.2	0.085	89
		3.5	2.6	0.045	33
		αPTB-IgG			
		6.5	0.4	0.005	87
		3.5	0.2	0.0025	31
EMCV	1.8	*Untreated*			
		8.0	8.8	0.08	100
		4.0	4.4	0.04	57
		Pre-im.-IgG			
		8.0	6.4	0.06	53
		4.0	3.2	0.03	28
		αPTB-IgG			
		8.0	0.5	0.005	44
		4.0	0.2	0.002	11
PV	0.36	*Untreated*			
		8.0	8.8	0.4	100
		4.0	4.4	0.2	65
		Pre-im.-IgG			
		8.0	6.4	0.3	22
		4.0	3.2	0.15	15
		αPTB-IgG			
		8.0	0.5	0.02	4.5
		4.0	0.2	0.009	0.9

[a]Ratio of translation products was quantitated by image analyzer.

Recent riboproteomic approach revealed the novel interacting proteins to IRESs [30], other than PTB, such as actin, forming homolog overexpressed in spleen, and microtuble interacting protein that associates with TRAF3. These factors should be characterized as novel ITAFs and comparative aspects in different IRESs should be addressed in the future work to clarify the character of each IRESs.

Acknowledgments

This work was supported by the grants from the Ministry of Health and Welfare, or Education, Culture, Sports, Science and Technology of Japan, the program for

promotion of fundamental studies in health sciences of the National Institute of Biomedical Innovation, and the Cooperative Research Project on Clinical and Epidemiological Studies of Emerging and Re-emerging Infectious Diseases.

References

[1] Choo QL, Kuo G, Weiner AJ, Overby LR, Bradley DW, Houghton M. Isolation of a cDNA clone derived from a blood-borne non-A, non-B viral hepatitis genome. Science 1989;244:359–62.
[2] Takamizawa A, Mori C, Fuke I, Manabe S, Murakami S, Fujita J, et al. Structure and organization of the hepatitis C virus genome isolated from human carriers. J Virol 1991;65:1105–13.
[3] Kato N, Hijikata M, Ootsuyama Y, Nakagawa M, Ohkoshi S, Sugimura T, et al. Molecular cloning of the human hepatitis C virus genome from Japanese patients with non-A, non-B hepatitis. Proc Natl Acad Sci USA 1990;87:9524–8.
[4] Kaito M, Watanabe S, Tsukiyama-Kohara K, Yamaguchi K, Kobayashi Y, Konishi M, et al. Hepatitis C virus particle detected by immunoelectron microscopic study. J Gen Virol 1994;75(Part 7):1755–60.
[5] Tsukiyama-Kohara K, Iizuka N, Kohara M, Nomota A. Internal ribosome entry site within hepatitis C virus RNA. J Virol 1992;66:1476–83.
[6] Kamoshita N, Tsukiyama-Kohara K, Kohara M, Nomoto A. Genetic analysis of internal ribosomal entry site on hepatitis C virus RNA: implication for involvement of the highly ordered structure and cell type-specific transacting factors. Virology 1997;233:9–18.
[7] Nomoto A, Tsukiyama-Kohara K, Kohara M. Mechanism of translation initiation on hepatitis C virus RNA. Princess Takamatsu Symp 1995;25:111–9.
[8] Pelletier J, Sonenberg N. Internal initiation of translation of eukaryotic mRNA directed by a sequence derived from poliovirus RNA. Nature 1988;334:320–5.
[9] Kieft JS, Zhou K, Jubin R, Doudna JA. Mechanism of ribosome recruitment by hepatitis C IRES RNA. RNA 2001;7:194–206.
[10] Yu Y, Ji H, Doudna JA, Leary JA. Mass spectrometric analysis of the human 40S ribosomal subunit: native and HCV IRES-bound complexes. Protein Sci 2005;14:1438–46.
[11] Hellen CU, Pestova TV, Litterst M, Wimmer E. The cellular polypeptide p57 (pyrimidine tract-binding protein) binds to multiple sites in the poliovirus 5′ nontranslated region. J Virol 1994;68:941–50.
[12] Hunt SL, Jackson RJ. Polypyrimidine-tract binding protein (PTB) is necessary, but not sufficient, for efficient internal initiation of translation of human rhinovirus-2 RNA. RNA 1999;5:344–59.
[13] Kolupaeva VG, Pestova TV, Hellen CU, Shatsky IN. Translation eukaryotic initiation factor 4G recognizes a specific structural element within the internal ribosome entry site of encephalomyocarditis virus RNA. J Biol Chem 1998;273:18599–604.
[14] Kolupaeva VG, Hellen CU, Shatsky IN. Structural analysis of the interaction of the pyrimidine tract-binding protein with the internal ribosomal entry site of encephalomyocarditis virus and foot-and-mouth disease virus RNAs. RNA 1996;2:1199–212.
[15] Sizova DV, Kolupaeva VG, Pestova TV, Shatsky IN, Hellen CU. Specific interaction of eukaryotic translation initiation factor 3 with the 5′ nontranslated regions of hepatitis C virus and classical swine fever virus RNAs. J Virol 1998;72:4775–82.
[16] Witherell GW, Wimmer E. Encephalomyocarditis virus internal ribosomal entry site RNA–protein interactions. J Virol 1994;68:3183–92.
[17] Scheper GC, Voorma HO, Thomas AA. Binding of eukaryotic initiation factor-2 and trans-acting factors to the 5′ untranslated region of encephalomyocarditis virus RNA. Biochimie 1994;76:801–9.
[18] Ali N, Siddiqui A. Interaction of polypyrimidine tract-binding protein with the 5′ noncoding region of the hepatitis C virus RNA genome and its functional requirement in internal initiation of translation. J Virol 1995;69:6367–75.
[19] Jang SK, Wimmer E. Cap-independent translation of encephalomyocarditis virus RNA: structural elements of the internal ribosomal entry site and involvement of a cellular 57-kDa RNA-binding protein. Genes Dev 1990;4:1560–72.

[20] Luz N, Beck E. Interaction of a cellular 57-kDa protein with the internal translation initiation site of foot-and-mouth disease virus. J Virol 1991;65:6486–94.
[21] Jang SK, Pestova TV, Hellen CU, Witherell GW, Wimmer E. Cap-independent translation of picornavirus RNAs: structure and function of the internal ribosomal entry site. Enzyme 1990;44:292–309.
[22] Garcia-Blanco MA, Jamison SF, Sharp PA. Identification and purification of a 62,000-Da protein that binds specifically to the polypyrimidine tract of introns. Genes Dev 1989;3:1874–86.
[23] Hiremath LS, Webb NR, Rhoads RE. Immunological detection of the messenger RNA cap-binding protein. J Biol Chem 1985;260:7843–9.
[24] Rau M, Ohlmann T, Morley SJ, Pain VM. A reevaluation of the cap-binding protein, eIF4E, as a rate-limiting factor for initiation of translation in reticulocyte lysate. J Biol Chem 1996;271:8983–90.
[25] Duncan R, Hershey JW. Identification and quantitation of levels of protein synthesis initiation factors in crude HeLa cell lysates by two-dimensional polyacrylamide gel electrophoresis. J Biol Chem 1983;258:7228–35.
[26] Flint SJ, Enquist LW, Krug RM, Racaniello VR, Skalka AM, editors. Virology. Washington, DC: ASM Press; 2000.
[27] Gingras AC, Svitkin Y, Belsham GJ, Pause A, Sonenberg N. Activation of the translational suppressor 4E-BP1 following infection with encephalomyocarditis virus and poliovirus. Proc Natl Acad Sci USA 1996;93:5578–83.
[28] Kaminski A, Jackson RJ. The polypyrimidine tract binding protein (PTB) requirement for internal initiation of translation of cardiovirus RNAs is conditional rather than absolute. RNA 1998;4:626–38.
[29] Hellen CU, Pestova TV. Translation of hepatitis C virus RNA. J Viral Hepat 1999;6:79–87.
[30] Lu H, Li W, Noble WS, Payan D, Anderson DC. Riboproteomics of the hepatitis C virus internal ribosomal entry site. J Proteome Res 2004;3:949–57.

Supplemental Material can be found at:
http://www.jbc.org/content/suppl/2009/11/13/M109.043232.DC2.html
http://www.jbc.org/content/suppl/2009/10/27/M109.043232.DC1.html
THE JOURNAL OF BIOLOGICAL CHEMISTRY VOL. 284, NO. 52, pp. 36442–36452, December 25, 2009

Hepatitis C Virus Impairs p53 via Persistent Overexpression of 3β-Hydroxysterol Δ24-Reductase*[S]

Received for publication, July 10, 2009, and in revised form, October 24, 2009 Published, JBC Papers in Press, October 27, 2009, DOI 10.1074/jbc.M109.043232

Tomohiro Nishimura[‡§1], Michinori Kohara[¶1], Kosuke Izumi[‖], Yuri Kasama[‡], Yuichi Hirata[¶], Ying Huang[‖2], Masahiro Shuda[¶3], Chise Mukaidani[**], Takashi Takano[¶], Yuko Tokunaga[‡], Hideko Nuriya[¶], Masaaki Satoh[‡], Makoto Saito[‡], Chieko Kai[‖], and Kyoko Tsukiyama-Kohara[‡4]

From the [‡]Department of Experimental Phylaxiology, Faculty of Medical and Pharmaceutical Sciences, Kumamoto University, 1-1-1 Honjo, Kumamoto, Kumamoto 860-8556, the [§]Chemo-Sero-Therapeutic Research Institute, Kikuchi Research Center, Kyokushi, Kikuchi, Kumamoto 869-1298, the [¶]Department of Microbiology and Cell Biology, Tokyo Metropolitan Institute of Medical Science, 1-6 Kamikitazawa 2-chome, Setagaya-ku, Tokyo 156-8506, the [‖]Laboratory Animal Research Center, Institute of Medical Science, University of Tokyo, 4-6-1 Shirokane-dai, Minato-ku, Tokyo 108-8639, and the [**]Study Service Department, PhoenixBio Company, Ltd., 3-4-1 Kagamiyama, Higashi-Hiroshima 739-0046, Japan

Persistent infection with hepatitis C virus (HCV) induces tumorigenicity in hepatocytes. To gain insight into the mechanisms underlying this process, we generated monoclonal antibodies on a genome-wide scale against an HCV-expressing human hepatoblastoma-derived cell line, RzM6-LC, showing augmented tumorigenicity. We identified 3β-hydroxysterol Δ24-reductase (DHCR24) from this screen and showed that its expression reflected tumorigenicity. HCV induced the DHCR24 overexpression in human hepatocytes. Ectopic or HCV-induced DHCR24 overexpression resulted in resistance to oxidative stress-induced apoptosis and suppressed p53 activity. DHCR24 overexpression in these cells paralleled the increased interaction between p53 and MDM2 (also known as HDM2), a p53-specific E3 ubiquitin ligase, in the cytoplasm. Persistent DHCR24 overexpression did not alter the phosphorylation status of p53 but resulted in decreased acetylation of p53 at lysine residues 373 and 382 in the nucleus after treatment with hydrogen peroxide. Taken together, these results suggest that DHCR24 is elevated in response to HCV infection and inhibits the p53 stress response by stimulating the accumulation of the MDM2-p53 complex in the cytoplasm and by inhibiting the acetylation of p53 in the nucleus.

Hepatitis C virus (HCV)[5] is composed of a single-stranded RNA genome of positive polarity (1). Translation of viral proteins is initiated from an internal ribosome entry site (2) and results in a single polypeptide that is subsequently cleaved by host and viral proteases to yield viable proteins (3). The HCV genome does not rely on canonical translation factors and can readily establish chronic infection without integrating into the host genome, resulting in hepatic steatosis and hepatocellular carcinoma (HCC) (4). More than 170 million people worldwide are infected with HCV (5); chronic HCV infection and aging are the major risk factors for HCC (6–8). Liver cancer is the fifth most common cause of cancer mortality worldwide (9). The frequent inactivation of p53 in human HCC suggests that the loss of p53-dependent apoptosis may promote hepatocarcinogenesis (10). Chronic HCV infection results in chronic liver inflammation and induces endoplasmic reticulum stress and oxidative stress, which are thought to induce hepatocarcinogenesis (11, 12). The mechanistic details underlying HCC development are not fully understood. To gain insight into the molecular mechanisms underlying HCV-induced pathogenesis, we previously established RzM6 cells (13), a human hepatoblastoma (HepG2)-derived cell line in which expression of the full-length HCV genome is controlled by a Cre/*loxP* system. Expression of the HCV genome promoted anchorage-independent growth of RzM6 cells after 44 days of culture from the onset of HCV expression (RzM6-44d cells) but not in RzM6 cells after 0 days (RzM6-0d cells) (13). In the present study, we generated monoclonal antibodies against RzM6 cells cultured for longer than 44 days (RzM6-LC cells) and then screened the antibodies for their ability to bind antigens overexpressed in these cells. We identified 3β-hydroxysterol Δ24-reductase (DHCR24) from this screen and characterized its role in the HCV-induced cell growth deregulation.

EXPERIMENTAL PROCEDURES

Cells, Growth Assay, and Plasmids—HepG2 human hepatoblastoma cells, HuH-7 human hepatoma cells, WRL68 human embryonic hepatic cells, HEK293 human embryonic kidney cells, and human WI38 fibroblast cells were purchased from the American Type Culture Collection. NIH3T3 mouse fibroplast cells were from Japanese Collection of Research Bioresource. Cells were cultured under the growth conditions described in the supplemental material. RzM6 cells were established by

* This work was supported by grants from the Ministry of Health and Welfare of Japan, the Ministry of Education, Culture, Sports, Science and Technology of Japan, the Program for Promotion of Fundamental Studies in Health Sciences of the National Institute of Biomedical Innovation, the Cooperative Research Project on Clinical and Epidemiological Studies of Emerging and Re-emerging Infectious Diseases, and the Hayashi Memorial Foundation for Female Natural Scientists.

[S] The on-line version of this article (available at http://www.jbc.org) contains supplemental Figs. 1–5.

[1] Both authors contributed equally to this work.

[2] Present address: Liver Diseases Branch, NIDDK, National Institutes of Health, Bethesda, MD 20892.

[3] Present address: Molecular Virology Program, University of Pittsburgh Cancer Institute, University of Pittsburgh, 5117 Centre Ave., Pittsburgh, PA 15213.

[4] To whom correspondence should be addressed. Tel.: 81-96-373-5560; Fax: 81-96-373-5560; E-mail: kkohara@kumamoto-u.ac.jp.

[5] The abbreviations used are: HCV, hepatitis C virus; HCC, hepatocellular carcinoma; siRNA, small interfering RNA; HA, hemagglutinin; ELISA, enzyme-linked immunosorbent assay; HBV, hepatitis B virus.

transfection of HepG2 cells with the plasmid *HCR6*-Rz, which contains the full-length HCV cDNA (nucleotides 1–9611; GenBank™ accession number AY045702), and stably transformed cell lines were selected in media containing G418 (800 μg/ml bioactive; Invitrogen). These cell lines, termed 2–18, were then transfected with pCAG-Mer-Cre-Mer (Cre/*loxP* system) and were selected in media containing puromycin (Sigma), as described previously (13), to generate the RzM6 cell line. HCV expression was induced by treatment with 4-hydroxy-tamoxifen (100 nM). Cells expressing HCV for 44 days (RzM6-44d cells) displayed augmented anchorage-independent cell growth. Cells expressing HCV for more than 44 days are referred to as RzM6-LC cells.

The tumor formation assay was performed by injecting RzM6-0d, RzM6-44d, or RzM6-LC cells in the exponential growth phase into nude mice. Cells in culture were harvested with trypsin, and 2×10^6 or 1×10^7 cells were subcutaneously injected into the backs of athymic nude mice (ICR strain, Charles River). HepG2 and WRL68 cells with plasmid DNA or small interfering RNA (siRNA) were transiently transfected using Lipofectamine 2000 or RNAi Max (Invitrogen). HepG2 cells transfected with the pcDNA3.1-based HA- and FLAG-tagged DHCR24 expression vector were selected in media containing 800 μg/ml G418 (Invitrogen). The terminal deoxynucleotidyltransferase-mediated dUTP nick end labeling assay was performed using the TMR red *in situ* cell death detection kit (Roche Applied Science).

Generation of Monoclonal Antibodies—BALB/c mice received seven or eight intraperitoneal injections of RzM6-44d cells (5×10^6 cells/injection) in RIBI adjuvant (trehalose dimycolate + monophosphoryl lipid A emulsion; RIBI ImmunoChemResearch) at 3–4-week intervals. At the end of this immunization regimen, the spleens were removed, and the splenocytes were fused with mouse myeloma PAI cells using polyethylene glycol 1500 (Roche Applied Science), as described previously (14). Hybridoma cells were selected in medium containing hypoxanthine, aminopterin, and thymidine (Invitrogen), and culture supernatants were collected for whole-cell enzyme-linked immunosorbent assay (ELISA) screening.

ELISA, Immunostaining, Northern Blotting, Western Blotting, and Immunoprecipitation—Immunofluorescence assays, whole-cell ELISA, standard ELISA, and immunostaining are described in the supplemental materials. Northern blotting was performed as described previously (13). For immunoprecipitation and Western blotting, frozen specimens were homogenized on ice using a Dounce homogenizer fitted with a type-A pestle (Wheaton Science Products) in radioimmune precipitation buffer (1% SDS, 0.5% (v/v) Nonidet P-40, 0.15 M NaCl, 10 mM Tris, pH 7.4, 5 mM EDTA, and 1 mM dithiothreitol). Western blotting was performed as previously described (13) with the following primary antibodies: anti-DHCR24 monoclonal antibody 2-152a, polyclonal anti-p53 (Cell Signaling Technologies), anti-MDM2 (murine double minute clone 2 oncoprotein) (Santa Cruz Biotechnology, Inc., Santa Cruz, CA), anti-Myc (9E10) (Santa Cruz Biotechnology, Inc.), and anti-HCV core protein monoclonal antibody 515 (15) or 31-2. Anti-p53 monoclonal antibody (DO-1) and polyclonal antibody (FL-393) (Santa Cruz Biotechnology, Inc.) were used for immunostaining. Phosphorylation of p53 was characterized by Western blotting with antibodies against phosphorylated Ser^6, Ser^9, Ser^{15}, Ser^{20}, Ser^{37}, Ser^{46}, and Ser^{329} (Cell Signaling Technologies). Acetylation of p53 was examined by immunoprecipitation with anti-p53 (DO-1) and the ExactaCruz immunoprecipitation reagent (Santa Cruz Biotechnology, Inc.), followed by Western blotting with antibodies against p53 (rabbit polyclonal; Cell Signaling) or acetylated p53 (Lys^{373}/Lys^{382}) (Upstate Biotechnology). The interaction between p53 and MDM2 was examined by immunoprecipitation with anti-p53 (FL-393) or anti-MDM2 (H221; Santa Cruz Biotechnology, Inc.) and protein A-Sepharose (GE Healthcare), followed by Western blotting with monoclonal antibodies against MDM2 (SMP14, Santa Cruz Biotechnology, Inc.) and p53 (DO-1), respectively. Polyclonal anti-actin (Santa Cruz Biotechnology, Inc.), anti-histone H1 (Santa Cruz Biotechnology, Inc.), and anti-heat shock protein 70 (HSP70) (Stressgen) primary antibodies were used for normalization of Western blots. Subcellular fractionation of RzM6-0d and LC cells was performed as previously described (15).

Cloning and Expression of DHCR24 and in Vitro Translation—Total RNA was isolated from 1×10^6 HuH-7 cells using ISOGEN Reagent (Nippon Gene). Purified RNA (2 μg) was reverse-transcribed with Superscript II (Invitrogen) using random primers according to the manufacturer's protocol. The DHCR24 cDNA was then amplified by PCR with Phusion DNA polymerase (BioLabs). The following primers were used for the first round of amplification: D-5-1 (5′-CCCGGGCTGTGGGCTACAGG-3′, forward) and D-3-1 (5′-CCAGGCCACTTTTATTTAAA-3′, reverse). Primers for the second round of amplification were D-5-2 (5′-GTTCTCGAGCAGTGACAGGAGGCGCGAAC-3′, forward) and D-3-2 (5′-GTTCTCGAGTCCAGGCGGGCTCCAGCTCA-3′, reverse). The amplified DHCR24 cDNA was subcloned into the pGEM-T easy vector (Promega). *In vitro* translation was performed using TNT(R) reticulocyte lysate (Promega) and the Express Protein Labeling Mix (New England Nuclear) in the presence of either [^{35}S]Met/Cys or non-radioactive methionine. Amplified DHCR24 cDNA was digested with XhoI and subcloned into the pCAG-PURO vector (16) for transfection into WRL68 cells using Lipofectamine 2000. Amplified DHCR24 cDNA was also subcloned into the pcDNA3.1 vector containing an HA or FLAG tag (kindly supplied by Dr. N. Takahashi, Tokyo University of Agriculture and Technology) for transfection into RzM6 or HepG2 cells using Lipofectamine LTX (Invitrogen). Transfected cells were selected in media containing G418.

The lentiviral vector, pCSII-EF-MCS-EMCV IRES-GFP (generous gift from Hiroyuki Miyoshi, RIKEN, Tsukuba, Japan), was modified by replacing the green fluorescent protein gene with the hygromycin phosphotransferase gene to construct pCSII-EF-MCS-EMCV IRES-Hygro. DHCR24 fused to the 5′-HA or 5′-FLAG tag-encoding sequence were cloned under the EF promoter. The resulting plasmid was cotransfected with packaging plasmid (pCAG-HIVgp and pCMV-VSVG-RSV-Rev) in 293FT cells (Invitrogen) to produce recombinant lentivirus. Following infection, cells were selected with hygromycin B (600 μg/ml; Sigma).

Silencing of DHCR24 and HCV by siRNA—The DHCR24 stealth siRNA was designed to target the human DHCR24 mRNA sequence 5′-GCAAGCUGAAUAGCAUUGGCAAUUA-3′ (nucleotides 970–993) using the BLOCK-iT RNAi designer (Invitrogen). A mutated siRNA (5′-GCAGUCUAACGAUUACGGAAAGUUA-3′) was synthesized as a control. An alternative siRNA, siDHCR24-1024, was designed as 5′-GAGAACUAUCUGAAGACAATT-3′. The HCV siRNA was synthesized as previously described (17). Cells were transfected with a 1 nM concentration of the chemically synthesized siRNAs using Lipofectamine 2000 or Lipofectamine RNAiMAX (Invitrogen) in Opti-MEM (Invitrogen) and then incubated for 4–6 h at 37 °C. Cells were characterized 48 h after transfection.

Caspase and Reporter Assays—Cells (1×10^4 cells/well) were seeded into white 96-well plates (Sumitomo Bakelite), treated with 1 mM H_2O_2, and then lysed with caspase-Glo 3/7 buffer (Promega). Caspase 3/7 activity was determined by measuring the absorbance resulting from cleavage of a proluminescent substrate containing the sequence DEVD (Promega) using a multilabel counter (PerkinElmer Life Sciences). The $p21^{WAF1/CIP1}$ promoter activity was assayed in HepG2, RzM6-0d, or RzM6-LC cells transfected with pWWP-Luc (kindly supplied by Dr. Bert Vogelstein (The Johns Hopkins University)). Cells were cotransfected with phRL-TK(Int-) (Promega) for normalization of promoter activity. Cells were incubated for 2 days after transfection and were then treated with 1 mM H_2O_2 for 4 h. Promoter activity was measured using the Dual-Luciferase reporter assay system (Promega).

HCV Infection of Humanized Chimeric Mouse Liver and mRNA Quantification by Quantitative Reverse Transcription-PCR—Detailed procedures are described in the supplemental material.

Statistical Analysis—Student's *t* test was used to test the statistical significance of the results. *p* values less than 0.05 were considered statistically significant.

RESULTS

Expression of DHCR24 Parallels Hepatocarcinogenesis—RzM6 cells expressing full-length HCV were established using the Cre/*loxP* expression-switching system (13). RzM6 cells cultured for longer than 44 days (termed RzM6-LC) had a greater ability to form colonies (13) and to induce tumors in nude mice (Fig. 1*A*). We produced monoclonal antibodies against RzM6-LC cells (see supplemental materials) and screened them for their ability to bind RzM6 antigens overexpressed upon the onset of hepatocarcinogenesis. Antibody clone 2-152a bound to a ~60-kDa protein (p60) that was expressed at higher levels in RzM6-LC cells than in RzM6 cells before the onset of HCV expression (termed RzM6-0d) (13) (Fig. 1*B*). p60 was strongly expressed in hepatoma-derived HuH-7 cells but was less abundant in the less aggressive cancer cell line, HepG2, or in the normal embryonic cell lines WRL68, HEK293, or NIH3T3 (supplemental Fig. 1*A*). To identify p60, the protein was purified from RzM6-LC cells using immunoaffinity chromatography and subjected to matrix-assisted laser desorption/ionization time-of-flight mass spectrometry (supplemental Fig. 1*B*). Through this process, p60 was identified as DHCR24 (also known as seladin-1) (18–20), an enzyme that catalyzes the reduction of the Δ-24 double bond of sterol intermediates during cholesterol biosynthesis and is up-regulated by oxidative stress (19, 21). DHCR24 cDNA was cloned and translated *in vitro* (Fig. 1*C*) and also expressed in human embryonic hepatic WRL68 cells (Fig. 1*D*), and the monoclonal antibody 2-152a reacted with the expressed protein (Fig. 1, *D* and *E*).

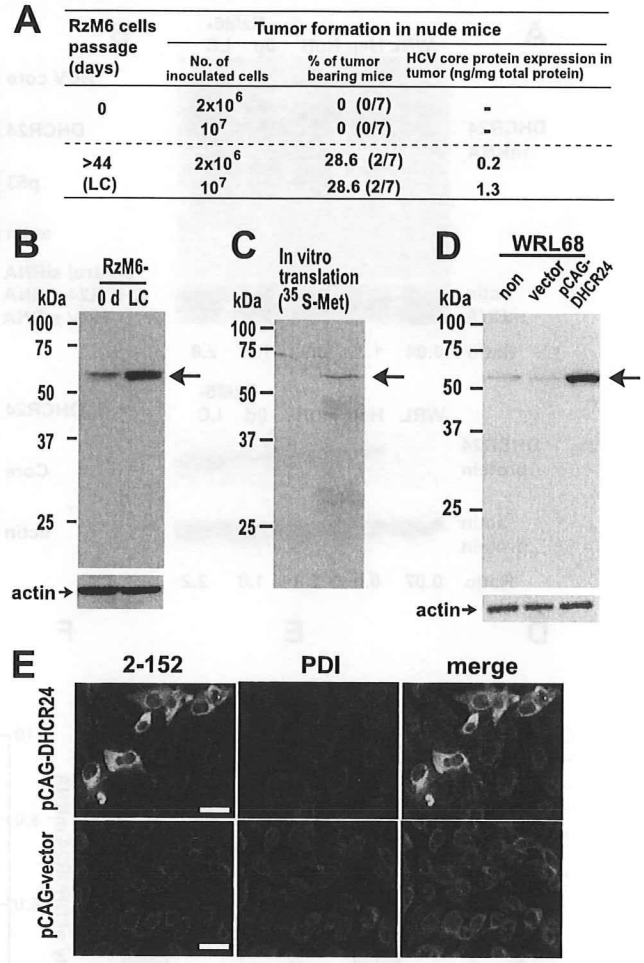

FIGURE 1. **Analysis of RzM6 cell tumorigenicity and identification of DHCR24 overexpression in RzM6-LC cells.** *A*, summary of tumor formation in nude mice injected with RzM6-0d or RzM6-LC cells. *B*, detection of a ~60-kDa protein (*arrow, upper panel*) in whole-cell lysates (30 μg/lane) from RzM6-0d and RzM6-LC cells by Western blotting with monoclonal antibody 2-152a. Anti-actin antibody was used for normalization (*arrow, lower panel*). Data are representative of two independent experiments. *C*, empty vector (pGEM3, *left lane*) or pGEM-DHCR24 (*right lane*) was subjected to *in vitro* transcription/translation using rabbit reticulocyte lysates in the presence of [^{35}S]methionine. Samples were subjected to SDS-PAGE followed by autoradiography. *D*, cell lysates from untransfected WRL68 cells (*non*), WRL68 cells transfected with empty pCAG vector (*vector*), and WRL68 cells transfected with pCAG-DHCR24 vector were examined by Western blotting with monoclonal antibody 2-152a (*upper panel*) or monoclonal anti-actin antibody (*lower panel*). *E*, WRL68 cells were transfected with pCAG-DHCR24 or pCAG vector alone and subjected to immunocytochemistry with monoclonal antibody 2-152a (*green*) or anti-protein-disulfide isomerase antibody (*PDI*; *red*). *Scale bars*, 25 nm.

HCV Induces Persistent DHCR24 Overexpression—Since DHCR24 was up-regulated in RzM6-LC cells, we examined whether HCV can induce DHCR24 expression in human hepatocytes. We also compared the expression levels of DHCR24